Lagrangian velocity correlation and spectrum in homogeneous isotropic turbulence

By T. Gotoh[1] R. S. Rogallo[2] AND J. R. Herring[3]

The Lagrangian velocity correlation and its spectrum are computed by direct numerical simulation (DNS) using the passive vector method (PVM), and the validity of the method is studied. It is found that the PVM is accurate when $K_{max}/k_d \geq 2$ where K_{max} is the maximum wavenumber carried in the simulation and k_d is the Kolmogorov wavenumber. The Eulerian and Lagrangian velocity correlations for various wavenumber bands are compared. At moderate to high wavenumber, the Eulerian velocity correlation decays faster than the Lagrangian, and the effect of sweep on the former is observed. The time scale of the Eulerian correlation is found to be $(kU_0)^{-1}$ and that of the Lagrangian to be $(\int_0^k p^2 E(p)dp)^{-1/2}$. The Markovianized Lagrangian renormalized approximation (MLRA) is compared to the DNS, and good agreement is found for one-time quantities in decaying turbulence at low Reynolds numbers and for the Lagrangian velocity autocorrelation in steady turbulence at moderate Reynolds number. The effect of intermittency on the Lagrangian correlation is discussed.

1. Introduction

The turbulent diffusion process is expressed naturally in terms of the Lagrangian velocity correlation, but the Lagrangian correlation is difficult to obtain from experiments or numerical simulations, whereas the Eulerian velocity correlation is easily obtained. Lagrangian information has traditionally been obtained from numerical simulations by tracking fluid particles which are released in the turbulent flow (Yeung & Pope 1988, 1989 and Squires & Eaton 1991). On the other hand, Kaneda & Gotoh (1991) and Gotoh & Kaneda (1991) proposed that the Lagrangian correlations be computed directly from initial velocity data that is carried within the Eulerian computation as a passive vector field with zero diffusivity. The Lagrangian velocity correlation is then simply the correlation between the current (Eulerian) velocity field and the passive vector (initial velocity) field. Since the absence of diffusivity in the passive-vector transport equation allows large gradients to develop in the passive vector field, accurate resolution at high wavenumbers is rapidly lost, and a k^2 equilibrium spectrum is formed there. Nevertheless the Lagrangian correlation can be accurately computed by the DNS provided that the passive vector is adequately resolved, and we have determined the resolution requirement empirically.

1 Permanent address: Department of Systems Engineering, Nagoya Institute of Technology, Japan

2 NASA Ames Research Center, Moffett Field, California, 94035, U.S.A.

3 National Center for Atmospheric Research, P.O.Box 3000, Boulder, Colorado 80307, U.S.A.

Yeung & Pope (1988) investigated the accuracy of a passive vector method in which the passive vector carried was the fluid-particle displacement from its initial position rather than its initial velocity. The resulting particle displacements would then have been used to calculate the initial particle velocities by interpolation within the initial velocity field, but the method was abandoned after it was found that the root-mean-square particle displacement error, for a specified set of particles, was much larger than that of the particle-tracking method. The error results not only from the effect of zero diffusivity but also from the interpolation required to evaluate the displacement of *specified* particles. While the numerical error resulting from the lack of diffusivity also contaminates the method used here, all interpolation is avoided by carrying the initial velocity itself as the passive vector field and by allowing the set of particles to vary with time.

There has been some controversy about the time scaling of the Eulerian and Lagrangian two-point two-time correlations and, in particular, about the sweeping effect that the large scale motion imposes on the Eulerian correlation at small scales (McComb & Shanmugasundaram 1984, Yakhot & Orszag 1986, Dannevik 1987, Yakhot et al. 1989, Chen & Kraichnan 1989). Resolution of this matter has been hindered by the lack of direct comparisons of the two correlations for given wavenumbers (Comte-Bellot & Corrsin 1971). Computation of the Lagrangian two-point two-time correlations allows us to compare the decay of the Eulerian and Lagrangian correlations for given wavenumbers and to examine their time scaling. The comparison confirms that at low to moderate Reynolds numbers, the decay of the Eulerian correlation at small scale is dominated by large-scale sweeping, with a time scale of $(kU_0)^{-1}$, while the Lagrangian correlation is dominated by strain and has a time scale of $(\int_0^k p^2 E(p)dp)^{-1/2}$.

Although one-time quantities, such as the energy spectrum, predicted by the statistical theories of turbulence have often been compared to data from DNS and/or experiments (eg. Gotoh et al. 1988), there have been far fewer comparisons of two-time quantities. We shall compare two-time correlations predicted by the MLRA theory (Kaneda 1981, Gotoh et al. 1988) with the DNS data. In steady turbulence at moderate Reynolds number, the one-point Lagrangian correlation predicted by the MLRA is in good agreement with the DNS. Intermittency effects will be illustrated by a short-time analysis of the correlation.

2. Basic equations

We assume that the Eulerian velocity $\mathbf{u}(\mathbf{x},t)$ and pressure $p(\mathbf{x},t)$ obey the Navier-Stokes equation for an incompressible fluid of unit density

$$\{\frac{\partial}{\partial t} + \mathbf{u}(\mathbf{x},t)\cdot\nabla\}\mathbf{u}(\mathbf{x},t) = -\nabla p(\mathbf{x},t) + \nu\triangle\mathbf{u}(\mathbf{x},t), \tag{2.1}$$

$$\nabla\cdot\mathbf{u}(\mathbf{x},t) = 0, \tag{2.2}$$

where ν is the kinematic viscosity. A generalized velocity field $\mathbf{v}(\mathbf{x},s|t)$ is defined (Kraichnan 1965) as the velocity at time t of the fluid particle that was at $\mathbf{x}$ at time

s. Note that $\mathbf{v}(\mathbf{x},t|t) = \mathbf{u}(\mathbf{x},t)$. The evolution of the velocity $\mathbf{v}(\mathbf{x},s|t)$ with respect to the *labeling time* s is governed by the labeling time transformation

$$\{\frac{\partial}{\partial s} + \mathbf{u}(\mathbf{x},s)\cdot\nabla\}\mathbf{v}(\mathbf{x},s|t) = 0. \tag{2.3}$$

The Lagrangian velocity auto-correlation R_L of a fluid particle that was at position $\mathbf{x}$ at time t_0 is defined by

$$R_L(\mathbf{x},t_0|t,s) \equiv < \mathbf{v}(\mathbf{x},t_0|t)\mathbf{v}(\mathbf{x},t_0|s) >, \tag{2.4}$$

where $<>$ denotes the ensemble average. If the turbulence is statistically homogeneous, R_L is independent of $\mathbf{x}$ and t_0 by the invariance properties of $\mathbf{v}(\mathbf{x},s|t)$ (Kraichnan 1965), and

$$\begin{aligned} R_L(t,s) \equiv R_L(\mathbf{x},t_0|t,s) &= \frac{1}{V}\int_V < \mathbf{v}(\mathbf{x},t_0|t)\mathbf{v}(\mathbf{x},t_0|s) > d\mathbf{x} \\ &= \frac{1}{V}\int_V < \mathbf{v}(\mathbf{x},s|t)\mathbf{v}(\mathbf{x},s|s) > d\mathbf{x} \\ &= \frac{1}{V}\int_V < \mathbf{u}(\mathbf{x},t)\mathbf{v}(\mathbf{x},t|s) > d\mathbf{x}, \end{aligned} \tag{2.5}$$

(for the derivation of (2.5), see Kaneda & Gotoh, 1991). This equation shows that if the turbulence is homogeneous, the *Lagrangian* velocity auto-correlation $R_L(t,s)$ can be obtained in terms of the *Eulerian* field $\mathbf{u}(\mathbf{x},t)$ (obtained by solving (2.1) and (2.2)) and the passive vector field $\mathbf{v}(\mathbf{x},t|s)$ (obtained by solving (2.3) with the *initial* condition $\mathbf{v}(\mathbf{x},s|s) = \mathbf{u}(\mathbf{x},s)$). In this article, we refer to the calculation of R_L using (2.5) as the passive vector method (Kaneda & Gotoh 1991, and Gotoh & Kaneda 1991).

3. The Lagrangian Spectrum in the PVM and its contamination

We define three spectra as follows;

$$\begin{aligned} < u_i(\mathbf{x},t)u_i(\mathbf{x}',t) > &= \int < u_i(\mathbf{k},t)u_i^*(\mathbf{k},t) > \exp(-i\mathbf{k}(\mathbf{x}-\mathbf{x}'))d\mathbf{k} \\ &= \int_0^\infty E(k,t)\sin kr/kr\ dk, \qquad r = |\mathbf{x}-\mathbf{x}'|, \end{aligned} \tag{3.1}$$

$$\begin{aligned} < v_i(\mathbf{x},t|s)v_i(\mathbf{x}',t|s) > &= \int < v_i(\mathbf{k},t|s)v_i^*(\mathbf{k},t|s) > \exp(-i\mathbf{k}(\mathbf{x}-\mathbf{x}'))d\mathbf{k} \\ &= \int_0^\infty E_P(k,t|s)\sin kr/kr\ dk, \end{aligned} \tag{3.2}$$

$$\begin{aligned} < u_i(\mathbf{x},t)v_i(\mathbf{x}',t|s) > &= \int < u_i(\mathbf{k},t)v_i^*(\mathbf{k},t|s) > \exp(-i\mathbf{k}(\mathbf{x}-\mathbf{x}'))d\mathbf{k} \\ &= \int_0^\infty E_L(k,t|s)\sin kr/kr\ dk, \end{aligned} \tag{3.3}$$

where the summation convention is used, homogeneity and isotropy of the turbulence are assumed, and * denotes complex conjugate. The first spectrum is the usual Eulerian energy spectrum, the second is the passive vector spectrum, and the third is the Lagrangian correlation spectrum. Note that the three spectra are identical at $t = s$.

Suppose that the velocity field $\mathbf{u}$ is computed from $t = 0$, and at time s we initialize the passive vector field $\mathbf{v} = \mathbf{u}$ and compute E_P and E_L as well as E for later times. Suppose also that we have infinite resolution, that is, the maximum resolved wavenumber K_{max} is infinite. Then the passive vector spectrum $E_P(k, t|s)$ will form a *viscous-convective* k^{-1} range (Batchelor 1959, Kraichnan 1968) with an ever increasing width as $(t - s)$ increases. What will happen when the numerical resolution is finite, say $K_{max} = 2k_d$? Until E_P becomes significant at the computational boundary K_{max}, the evolution of E_P is identical to that for infinite K_{max}, and there is no contamination in E_P. Eventually the error at $E_P(K_{max})$ builds and propagates to lower wavenumber. The time t_d at which $E_P(K_{max})$ becomes significant is given roughly by the Kolmogorov time scale $t_d = (\epsilon/\nu)^{-1/2}$ (Batchelor 1959, Kraichnan 1968), and the contamination will reach the lower bands at k_d at $t - s \sim 2t_d$. Now consider the evolution of $E_L(k, t|s)$. The quantity $< u_i(\mathbf{k}, t)v_i^*(\mathbf{k}, t|s) >$ may be written as

$$< u_i(\mathbf{k},t)v_i^*(\mathbf{k},t|s) > =< |u_i(\mathbf{k},t)||v_i^*(\mathbf{k},t|s)| \ \exp[-i\{\phi_i^u(\mathbf{k},t) - \phi_i^v(\mathbf{k},t|s)\}] >, \quad \text{(no summation)}$$

where $\phi_i^u(\mathbf{k}, t)$ and $\phi_i^v(\mathbf{k}, t|s)$ are the phases of the Fourier components $\mathbf{u}(\mathbf{k}, t)$ and $\mathbf{v}(\mathbf{k}, t|s)$, respectively. This implies that the magnitude of $< u_i(\mathbf{k}, t)v_i^*(\mathbf{k}, t|s) >$ is roughly proportional to $\sqrt{E(k,t)E_P(k,t|s)}/4\pi k^2$. When $t_d \leq t - s \leq 2t_d$, $E_P(k, t|s)$ for $k_d \leq k \leq K_{max}$ is at most of order k^2, and for $k \leq k_d$ is the same as it would be for the infinite K_{max}. Therefore the error in R_L caused by contamination of E_L at high wavenumbers is very small provided that $E(k, t)$ falls off rapidly at wavenumbers higher than k_d (meaning that the velocity field $\mathbf{u}$ remains well resolved). The above argument considers only the magnitude, thus it gives the upper bound of contamination of E_L. If $K_{max} = k_d$, the contamination and decay of the correlation occur simultaneously after $t = s$, and the effect of finite K_{max} becomes serious if the kinetic energy spectrum is broad. The requirement for accuracy of the PVM is thus $K_{max}/k_d \geq 2$ and is much more severe than that of Yeung and Pope (1988) who found the condition for accuracy of the particle tracking method (using cubic-spline interpolation) to be $K_{max}/k_d \geq 1$.

4. Computation of R_L for decaying turbulence

To test the validity of the PVM, we computed R_L in decaying turbulence for two types of initial spectra:
spectrum A

$$E(k) = 32(2/\pi)^{1/2}u_0^2k_p^{-5}k^4\exp[-2(k/k_p)^2], \qquad u_0 = 1 \text{ and } k_p = 4.75, \qquad (4.1)$$

Run	time	ν	E		Ω		R_λ		k_d		K_{max}
			DNS	MLRA	DNS	MLRA	DNS	MLRA	DNS	MLRA	
CRAY											
A	t=0	.01187	3.0	3.0	84.9	84.9	35.4	35.4	27.9	27.9	15, 30, 60
	s=0.861	.01187	1.23	1.19	58.9	57.1	17.4	17.0	25.4	25.2	15, 30, 60
INTEL											
AH	t=0	.01187	3.0	3.0	84.9	84.9	35.4	35.4	27.9	27.9	60
	s=1.16	.01187	0.872	0.848	38.5	35.3	15.3	15.5	22.9	22.4	60
BH	t=0	.01	2.93	2.87	162	162	29.7	29.1	35.7	35.7	30, 60
	s=0.667	.01	1.52	1.45	63.0	63.8	24.7	23.4	28.2	28.3	30, 60
SH*		.01	13.0	13.0	1330	1420	46.1	44.5	60.4	61.4	60

Table 1. Numerical data for DNS and MLRA

* The values of DNS are averages over the time span $0 \leq t - s \leq 0.586$.

spectrum B

$$E(k) = 3u_0^2 k_p^{-2} k \exp[-k/k_p], \qquad u_0 = 1 \text{ and } k_p = 3.0. \tag{4.2}$$

The various numerical data are summarized in table 1. In the DNS, the Navier Stokes equation is solved by a pseudospectral method in which wave-space truncation and phase shifting are used to remove the aliasing error (Rogallo 1981). The computations were begun on a Cray YMP and subsequently moved to an Intel Gamma (Hypercube) parallel machine. The time advance used on the Cray was fourth-order Runge-Kutta, and second-order Runge-Kutta was used on the Intel.

Figures 1 to 4 display the one-time data for runs with $K_{max} = 60$. The Kolmogorov wavenumber k_d at time s is 25.4 and 28.2 respectively, so that the velocity fields are well resolved. Figures 1 and 2 show the decay of total enstrophy for spectra A and B respectively. The dotted curves indicate the evolution for linear (viscous) decay. The spectra at time s are presented in figures 3 and 4.

The octave-band Lagrangian correlations and their partial sums are defined as

$$\widehat{R}_L^l(t,s) = \frac{\sum\limits_{oct} < u_i(\mathbf{k},t) v_i^*(\mathbf{k},t|s) >}{\left\{\sum\limits_{oct} < |u_i(\mathbf{k},t)|^2 >\right\}^{1/2} \left\{\sum\limits_{oct} < |v_i(\mathbf{k},t|s)|^2 >\right\}^{1/2}}, \tag{4.3}$$

$$\overline{R}_L^l(t,s) = \frac{\sum\limits_{k=1}^{min[2^{l+1},K_{max}]} < u_i(\mathbf{k},t) v_i^*(\mathbf{k},t|s) >}{\sqrt{E(t)E(s)}}, \tag{4.4}$$

where $\sum_{oct} \equiv \sum_{k=2^l}^{min[2^{l+1},K_{max}]}$. The correlation $\widehat{R}_L^l$ provides a measure of the phase error for each wavenumber band, while the partial sum $\overline{R}_L^l$ indicates the numerical

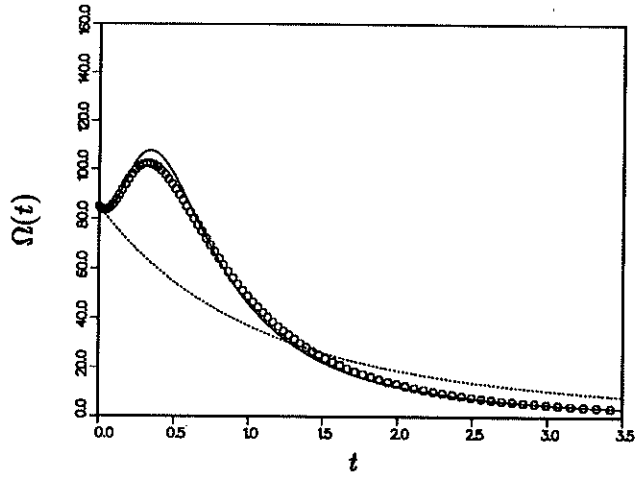

FIGURE 1. Evolution of the total enstrophy for run A.
—— MLRA, o DNS, ····· Linear decay.

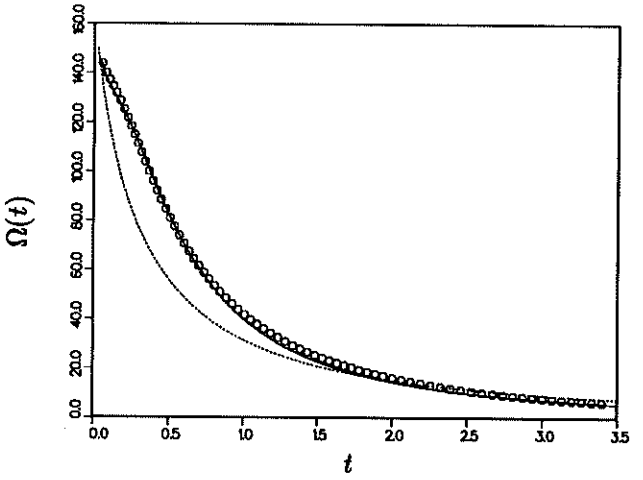

FIGURE 2. Evolution of the total enstrophy for run BH.
—— MLRA, o DNS, ····· Linear decay.

convergence of the contributions of the wavenumber bands to the total correlation. The accuracy of the PVM is examined as follows. Compute the velocity field $\mathbf{u}(\mathbf{x}, t)$ with $K_{max} = 60$ from $t = 0$ to $t = s$ when the turbulence is fully developed. For times $t > s$ compute $\widehat{R}_L^l(t, s)$ and $\overline{R}_L^l(t, s)$ by the PVM for several different numerical resolutions K_{max}. Figures 5 to 8 show $\widehat{R}_L^l(t, s)$ and $\overline{R}_L^l(t, s)$ for runs A and B respectively. The accuracy requirement for the PVM, $K_{max}/k_d \geq 2$, is satisfied in runs A and BH since k_d at time s is 25.4 and 28.2 respectively. It should be noted that the runs with $K_{max} = 30$, in which $K_{max}/k_d = 1.18$ for run A and 1.06 for run BH, yield almost the same results as those having $K_{max} = 60$. For the

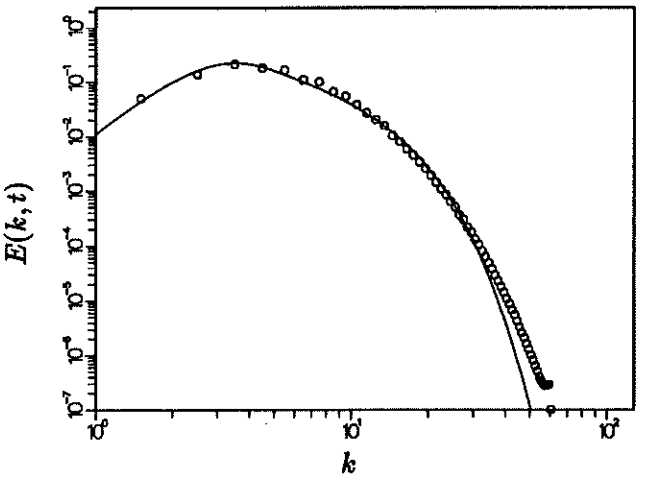

FIGURE 3. Comparison of the energy spectrum at $s = 0.861$ for run A. —— MLRA, o DNS.

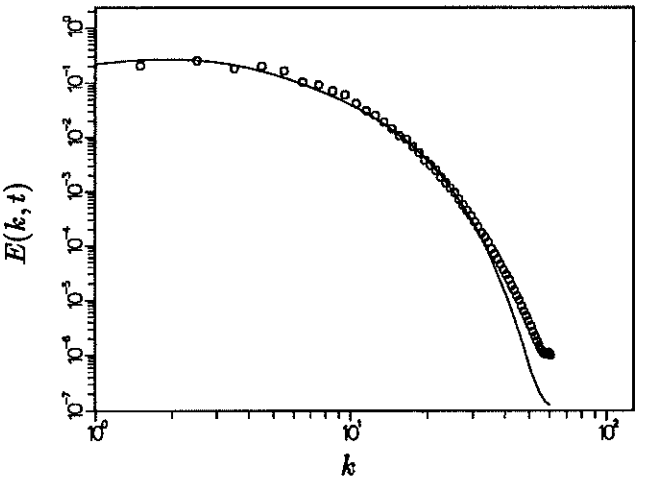

FIGURE 4. Comparison of the energy spectrum at $s = 0.667$ for run BH. —— MLRA, o DNS.

one-point Lagrangian correlation $R_L(t,s)$, even run A with $K_{max} = 15 = 0.59k_d$ is satisfactory when compared to that of $K_{max} = 60$ (see figure 6) because $R_L(t,s)$ is dominated by the energy containing scales $1 \leq k \leq 8$ which contribute about 80% of the total correlation at time s. The decorrelation time t_d at time s is about 0.13 for both runs A and BH and is seen to be shorter, roughly by a factor 2, than the decay time of $\widehat{R}_L^l(t,s)$ for the highest octave band $32 \leq k \leq 60$ (figures 5 and 7). This is consistent with the rapid decay of total enstrophy.

Figures 9 and 10 present the evolution of $E_P(k,t|s)$ and $E_L(k,t|s)$ respectively for run BH. In figure 10 data is omitted for wavenumbers where $\widehat{R}_L(k,t,s)$ is less than 0.05 to remove the statistical fluctuation. The passive vector spectrum $E_P(k,t|s)$

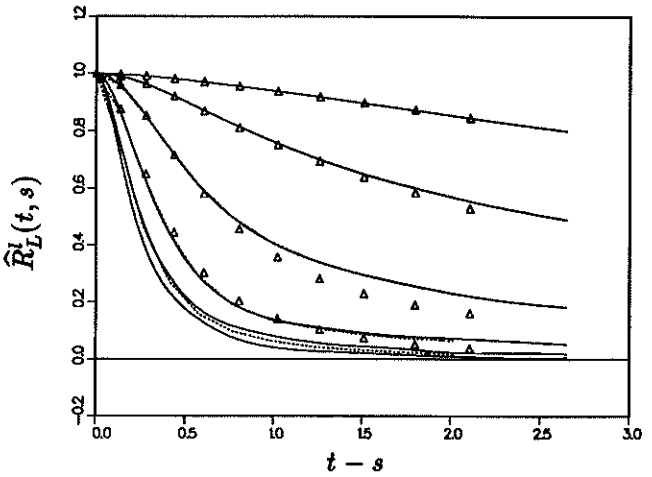

FIGURE 5. Lagrangian correlation within octave bands for run A. The uppermost curve corresponds to the lowest octave and the correlation decreases monotonically for successive octaves.
—— $K_{max} = 60$, ····· $K_{max} = 30$, ▵ $K_{max} = 15$.

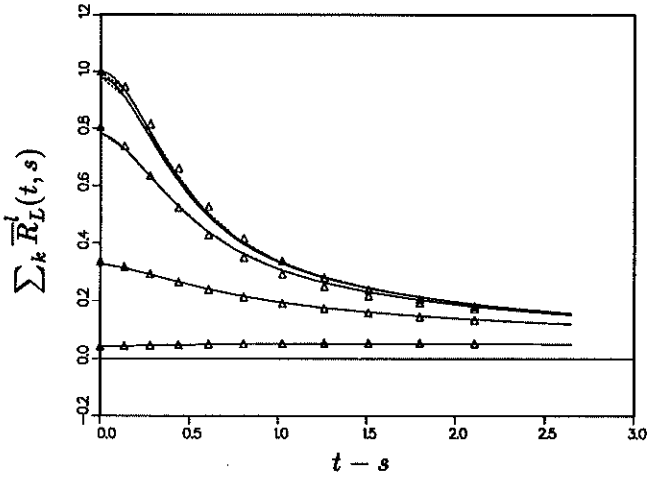

FIGURE 6. Contribution of octave bands to $R_L(t,s)$ for different K_{max} for run A. The lowermost curve corresponds to the lowest octave, and the partial sum increases monotonically with the addition of successive octaves.
—— $K_{max} = 60$, ····· $K_{max} = 30$, ▵ $K_{max} = 15$.

near K_{max} increases with time $t - s$ and for the band $10 \leq k \leq 20$ becomes approximately k^{-1} for a period of time during which $E_L(k, t|s)$ decays rapidly in the high wavenumber range.

5. Comparison of the Lagrangian and Eulerian correlation spectra

There have been previous investigations of the time scaling of the Eulerian and

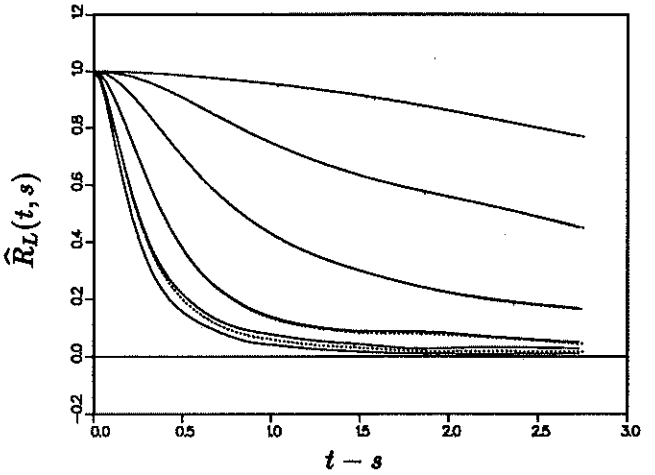

FIGURE 7. The same as in figure 5 but for run BH.
—— $K_{max} = 60$, ····· $K_{max} = 30$.

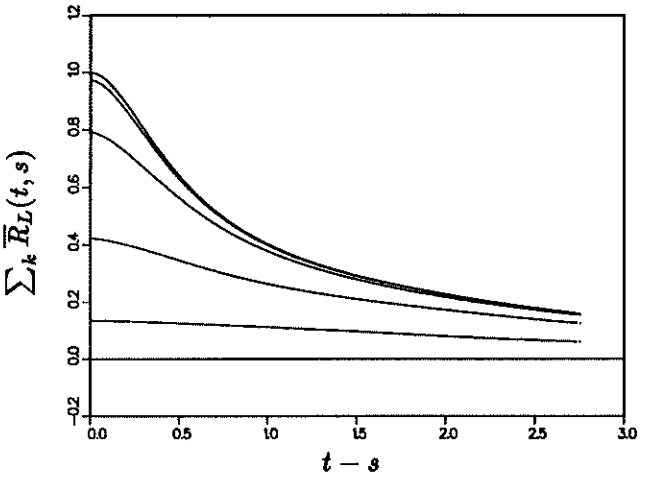

FIGURE 8. The same as in figure 6 but for run BH.
—— $K_{max} = 60$, ····· $K_{max} = 30$.

Lagrangian two-point two-time correlations, but there seems to remain some controversy, especially about the sweeping effect in the Eulerian correlation (McComb & Shanmugasundaram 1984, Yakhot & Orszag 1986, Dannevik 1987, Yakhot et al. 1989, Chen & Kraichnan 1989). Since one reason for the dispute seems to be the lack of appropriate data, it is very useful and interesting to compare the Eulerian and Lagrangian correlations at various spatial scales.

Figures 11 and 12 compare the decay of the Eulerian and Lagrangian correlations within octave bands for DNS runs A and BH, respectively. The Eulerian correlation is defined similarly to (4.3). In spite of the low Reynolds numbers, the Eulerian correlations for bands $k \geq 2$ decay faster than the Lagrangian, while the Eulerian

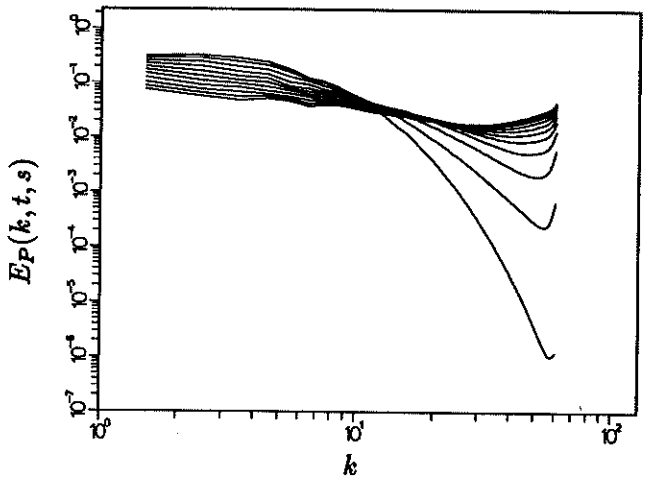

FIGURE 9. Evolution of the passive vector energy spectrum after $s = 0.6674$ for run BH.

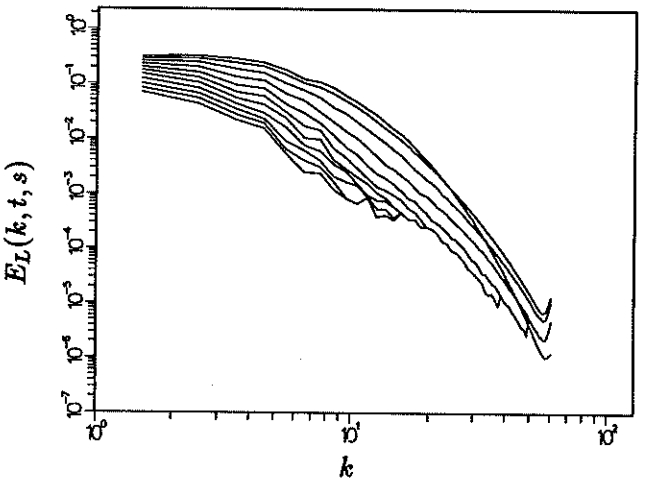

FIGURE 10. Evolution of Lagrangian spectrum after $s = 0.6674$ for run BH.

correlation for the band $1 \leq k \leq 2$ decays slower than the Lagrangian. Similar results are found for steady turbulence (forced run SH at $R_\lambda = 46$, figure not shown). This suggests that sweeping by large scales dominates the decay of the Eulerian correlation at small scales irrespective of Reynolds number.

Figures 13 and 14 present the time-scaled evolution of the Eulerian and Lagrangian correlations from run SH for several wavenumbers. The collapse of the curves is satisfactory, and a similar collapse is found for runs A and BH (figures not shown). The Eulerian characteristic time is $\tau_E = (kU_0)^{-1}$, the sweeping time of scale k^{-1} by the velocity intensity U_0. The Lagrangian characteristic time is $\tau_L = \{\int_0^k dpp^2 E(p,t)\}^{-1/2}$, the time for deformation of scale k^{-1} by all larger scales.

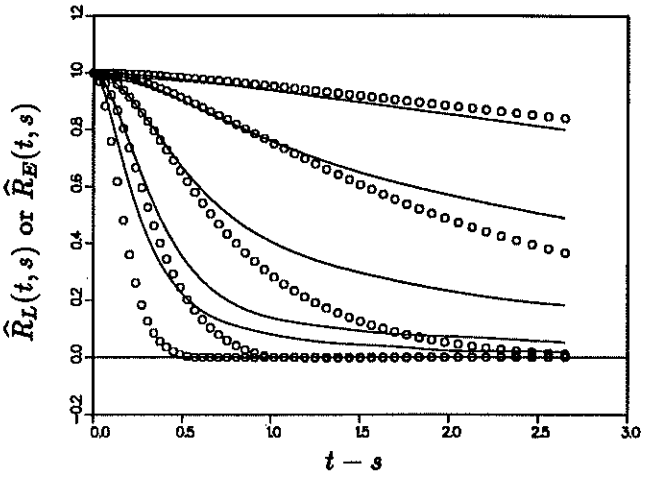

FIGURE 11. Comparison of decay of $\widehat{R}_L(t,s)$ and $\widehat{R}_E(t,s)$ for run A. Octave bands are $2^n < k < 2^{n+1}, n = 0,\cdots,4$ and $32 < k < 60$ from the uppermost line, respectively. —— $\widehat{R}_L(t,s)$, o $\widehat{R}_E(t,s)$.

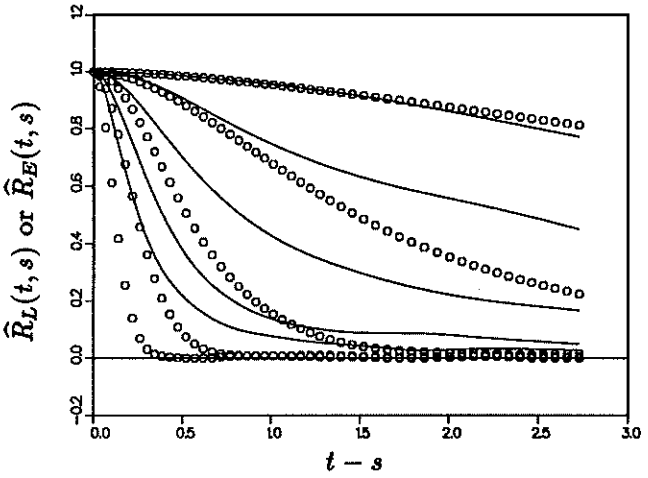

FIGURE 12. The same as in figure 11 but for run BH.

6. Comparison with the two-point closure theory

The LRA (Lagrangian Renormalized Approximation, Kaneda 1981) and the MLRA (Markovianized LRA) are Galilean invariant closures that give a $k^{-5/3}$ inertial-range spectrum and contain no adjustable parameters, but which are much simpler than the LHDIA closure of Kraichnan (1965). The predictions of the LRA and MLRA agree well with DNS results, especially the MLRA which satisfies the requirement of realizability (Gotoh, et al. 1988). The LRA and MLRA derivations and their equations are found in Kaneda (1981) and Gotoh et al. (1988). In what follows, we shall compare the MLRA and DNS results.

For the one-time quantities (figures 1 to 4), the agreement of the MLRA with

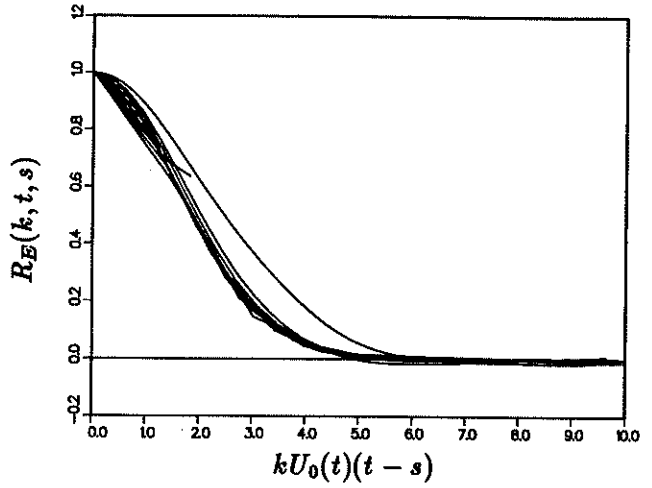

FIGURE 13. Time-scaled Eulerian correlations for bands $k = 2 + 5n$, $n = 1, \cdots, 11$ for run SH. $U_0 = \sqrt{E/3}$.

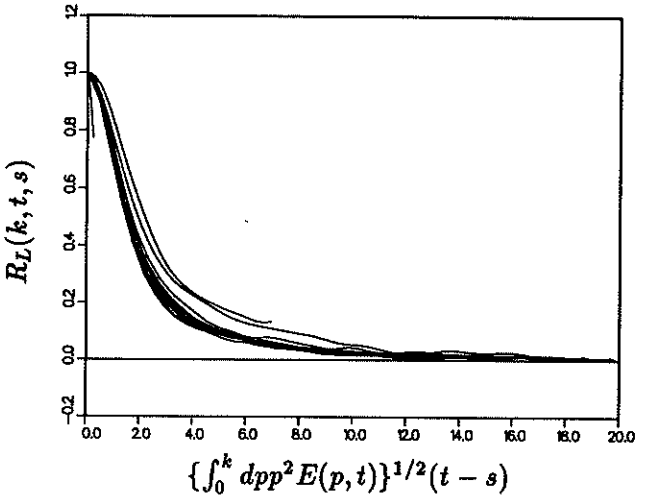

FIGURE 14. Time-scaled Lagrangian correlations for bands $k = 2 + 5n$, $n = 1 \cdots 11$ for run SH.

the DNS is satisfactory. Figures 15 and 16 show the comparison of the one-point Lagrangian correlation defined by

$$R_L^{bare}(t,s) = \frac{\sum_{\mathbf{k}} < u_i(\mathbf{k},t) v_i^*(\mathbf{k},t|s) >}{E(s)}, \tag{6.1}$$

where $\sum_{\mathbf{k}} \equiv \sum_{k=1}^{K_{max}}$, for runs A and BH, respectively.

The agreement between the MLRA and DNS for this two-time correlation is not as good as that for the one-time quantities. The difference seems to be due in part

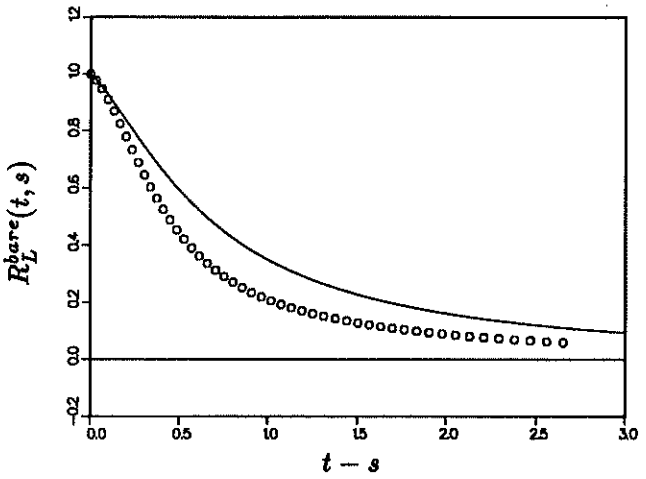

FIGURE 15. Comparison of the MLRA and the DNS for the $R_L^{bare}(t,s)$ for run A. —— MLRA, o DNS. $s = 0.86077$.

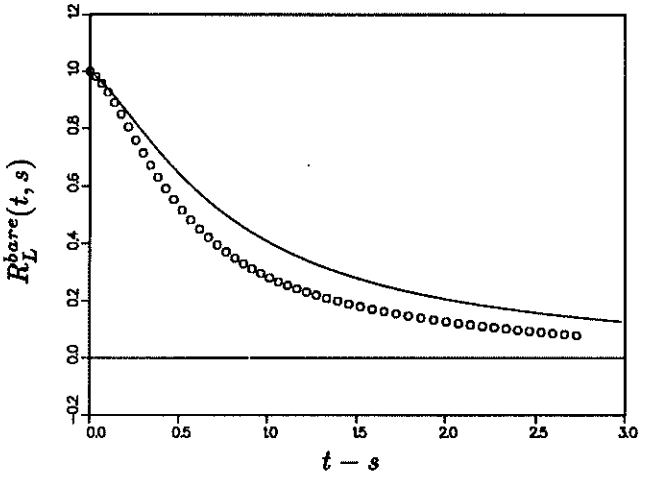

FIGURE 16. The same as in figure 15 but for run BH. $s = 0.6674$.

to the low values of R_λ. The effect of intermittency is discussed in the next section. To see the effect of the Reynolds number and to remove the direct effect of energy decay, we carried out a DNS of steady turbulence in which forcing was provided by the addition of an instability term to the Navier Stokes equation,

$$(\frac{\partial}{\partial t} + \nu k^2 - \alpha(k,t))u_i(\mathbf{k},t) = M_{ilm}(\mathbf{k}) \sum_{\mathbf{k}=\mathbf{p}+\mathbf{q}} u_l(\mathbf{p},t)u_m(\mathbf{q},t). \tag{6.2}$$

$$\alpha(k,t) = \begin{cases} c(t), & \text{for } 4 \le k \le 8; \\ 0, & \text{otherwise.} \end{cases} \tag{6.3}$$

The coefficient $c(t)$ is determined such that $\gamma = k_d(t)/K_{max} = (\epsilon(t)/\nu^3)^{1/4}/K_{max}$ remains constant throughout the computation. The energy balance gives

$$c(t) = \frac{2\nu \int_0^\infty k^2 E(k,t)dk}{2\int_4^8 E(k,t)dk} = \frac{\epsilon(t)}{2\int_4^8 E(k,t)dk} = \frac{\nu^3(\gamma K_{max})^4}{2\int_4^8 E(k,t)dk}. \tag{6.4}$$

In a steady state, $c(t)$ is statistically constant in time, with a very small deviation. The criterion for the accuracy of the PVM requires $\gamma \leq 0.5$, but we were limited by computer capacity to $\gamma = 1$ because we desired both that the Reynolds number be large and that the forced wavenumber band be high enough ($4 \leq k \leq 8$) to avoid large fluctuations due to a small number of forced modes. Recall that in the decaying runs A and BH the one-point Lagrangian correlations computed with $\gamma \sim 1$ are not appreciably different from those computed with $\gamma \leq 0.5$ ($K_{max} = 60$). In the MLRA computation for run SH only the response equation was solved, using the (steady) energy spectrum from the DNS. Note that MLRA is equivalent to LRA when the turbulence is steady.

Figure 17 shows the energy spectra of DNS run SH and the averaged spectrum used in the MLRA calculation. The Reynolds number R_λ is about 46 in the DNS and $k_d = 60.4$ as expected. In figure 18, which compares R_L from the MLRA and DNS, we have compensated for the small difference in the total enstrophy between the DNS and MLRA by normalizing time by the root of the total enstrophy. The agreement seems satisfactory and suggests that the MLRA would yield a good prediction for the Lagrangian correlation at high Reynolds numbers.

7. Effects of intermittency

To investigate the reason for the relatively poor prediction of $R_L(t,s)$ by the MLRA in the low-Reynolds-number-decay runs A and BH, a small time analysis of the Lagrangian correlation is useful. Taylor expansion of $R_L(t,s)$ at $t = s$ gives

$$R_L(t,s) = C_0 + C_1(t-s) + \frac{1}{2}C_2(t-s)^2 + \cdots. \tag{7.1}$$

When $\nu = 0$, $C_1 = 0$ and

$$C_2 = \frac{1}{V}\int < u_{j,i}(\mathbf{x},s)u_{i,j}(\mathbf{x},s)G(\mathbf{x}-\mathbf{y})u_{l,m}(\mathbf{y},s)u_{m,l}(\mathbf{y},s) > d\mathbf{y}, \tag{7.2}$$

where G is the Green's function of the Laplace operator. The curvature C_2 depends on fourth-order moments of the velocity derivatives. The MLRA uses the nearly-Gaussian assumption for the velocity fields so that the fourth-order moments are expressed in terms of second-order moments. Three values of the curvature of R_L at $t = s$ are presented in table 2: a) C_2^{DNS}, computed by DNS with zero viscosity from the fully developed turbulence field, b) $\overline{C}_2^{DNS}$, computed by DNS with zero viscosity from a gaussian turbulence field (with the same energy spectrum as that for C_2^{DNS}), and c) C_2^{MLRA}, computed by the MLRA.

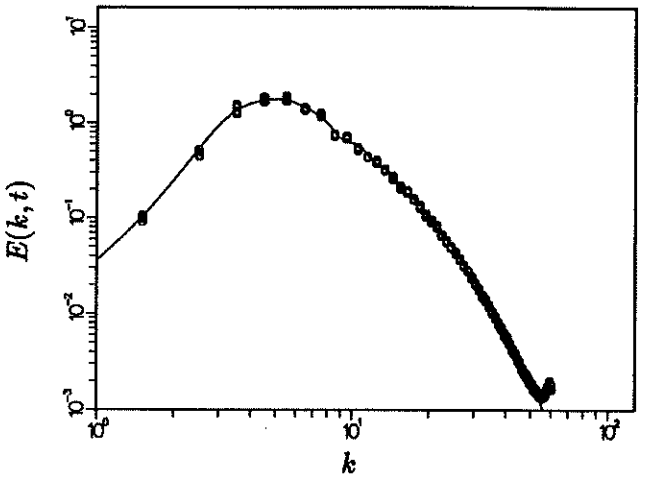

FIGURE 17. Energy spectrum for run SH. The spectra from the DNS are shown at 200 step intervals during the time span of $R_L(t-s)$. o DNS, and —— the spectrum used in the MLRA (time averaged DNS energy spectrum).

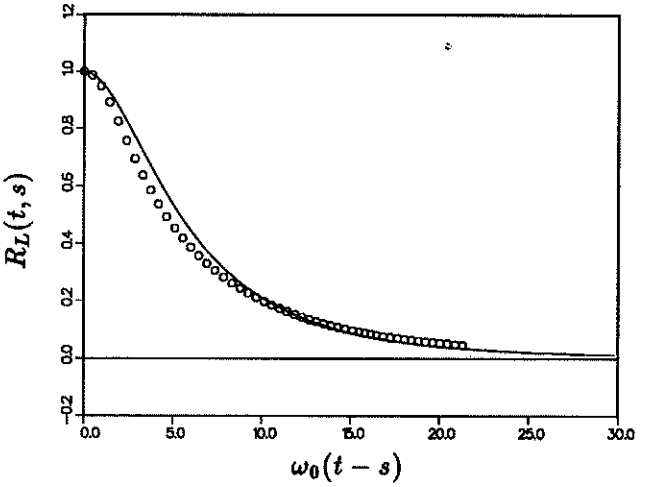

FIGURE 18. Comparison of $R_L(t,s)$ for the MLRA and DNS. —— MLRA, o DNS.

Run	time	C_2^{DNS}	$\overline{C}_2^{DNS}$	C_2^{MLRA}
AH	s=1.16	4.33	3.17	2.69
BH	s=0.667	9.76	7.11	6.61

Table 2. Curvature of R_L at $t = s$ from DNS and MLRA.

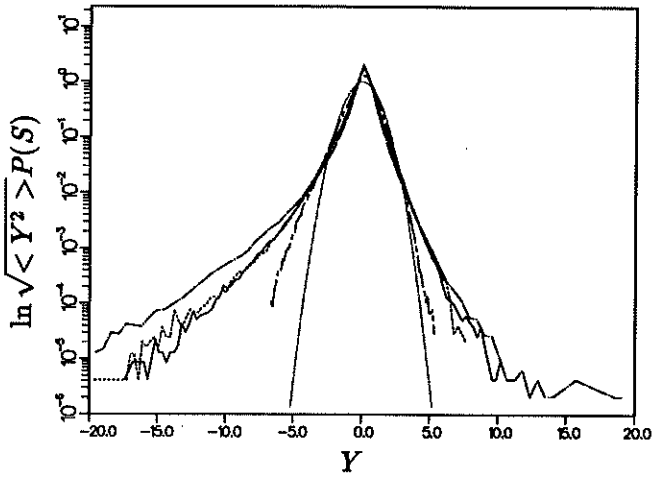

FIGURE 19. The PDF of $Y = (u_{i,j})^2 - <(u_{i,j})^2>$ at $t = s$. —— MLRA, — — — run AH($t = \delta t$), - - - - run BH, —·— run SH, ····· Gaussian.

It is found that $C_2^{MLRA}/C_2^{DNS} = 0.62$ for run A and 0.67 for run BH, while $C_2^{MLRA}/\overline{C}_2^{DNS} = 0.84$ for run A and 0.93 for run BH. The latter two values differ from unity in spite of the fact that the MLRA and DNS velocity fields both have random phases and Gaussian statistics. This is due to the difference between the energy spectra (more precisely, $k^2E(k,s)$) of the MLRA and DNS at $t = s$ and to the use of zero viscosity in the DNS. Values of C_2^{DNS} larger than Gaussian values imply intermittency of the velocity gradients. In fact, the PDF of the transverse velocity gradient is not Gaussian (figures not shown) as found in recent studies (She et al. 1988). Equation (7.2) implies that the curvature C_2 depends on the statistics of $S(\mathbf{x}) \equiv u_{j,i}(\mathbf{x})u_{i,j}(\mathbf{x})$ rather than the transverse velocity gradient itself and is related to the nonlinear coupling through the pressure term of the Navier Stokes equation. Figure 19 shows the PDF of $Y \equiv S - <S>$ for runs A ($t = \delta t$ and s), BH ($t = s$) and SH ($t = s$). The PDF's are non Gaussian and skewed. It should be noted that for small Y the three PDF's at $t = s$ are nearly equal.

Since the Reynolds numbers for runs A and BH are relatively low, the inertial and dissipation ranges are not separated, and the intermittency effect observed in the Lagrangian curvature C_2 is a mixture of the intermittencies in both ranges, but it is dominated by that of the dissipation range. It should be noted that the integrand of (7.2) contains the Green's function for the Laplacian operator, thus the contributions to C_2 would have a peak between the energy containing and dissipation ranges when the Reynolds number is sufficiently high, and the intermittency effect on C_2 would be primarily that of the inertial range with a smaller contribution from the dissipation range (She et al. 1988). At high Reynolds number, we expect the MLRA to give a better prediction for R_L, but the values for run SH ($R_\lambda = 46$) are already in reasonable agreement with the DNS.

It is surprising that for runs A and BH the one-time statistics from the MLRA are in good agreement with the DNS while the two-time quantities are not. Poor

prediction of $R_L(t,s)$ suggests poor values of Lagrangian covariances such as $< u_i(\mathbf{k},t)v_j^*(\mathbf{k},t|s) >$ that appear in the expression for the energy transfer function and that, in turn, would suggest poor prediction of one-time quantities such as total energy, energy spectrum, etc. There are several possible solutions to this paradox: first, at low Reynolds number, the energy transfer may be relatively unimportant for $t > s$, and second , the nonlinear coupling of the Navier Stokes equation is insensitive to the detail of the Lagrangian covariance for the energy transfer. In order to get more insight into this robustness in the energy transfer, it would be necessary and interesting to examine the Lagrangian correlation spectrum for each wavenumber. However, the two-point Lagrangian correlations from the PVM do not correspond to those of the MLRA but rather to those of the ALHDIA (Kraichnan 1965, 1966).

8. Discussion

The passive vector method in 3-D homogeneous isotropic turbulence can be used to compute the Lagrangian velocity auto-correlation function R_L as well as its spectrum. However, the numerical resolution requirement for its accuracy, $K_{max}/k_d \geq 2$, is much more severe than that, $K_{max}/k_d \geq 1$, of the particle tracking method. The PVM is very expensive because carrying a passive vector in the computation while doubling K_{max} requires roughly $2^3 \times 2 = 16$ times more memory and 32 times more cpu time than that needed to compute the velocity field alone versus less than two times more for the particle tracking method. On the other hand, the PVM has a much larger sample of particles and gives direct access to two-point two-time correlations. In addition, the implementation of the method is trivial when compared to particle tracking, especially on the new generation of parallel computers that utilize distributed memory. The Lagrangian correlation spectrum can be used to study the time scales associated with small scales. In fact, the Eulerian and Lagrangian time scales are found to be $(kU_0)^{-1}$ and $(\int_0^k p^2 E(p)dp)^{-1/2}$, respectively. Thus the sweeping effect by the large scale motion dominates the decorrelation of the Eulerian correlation at high wavenumbers.

It is found that at moderate Reynolds number the MLRA is more accurate than LRA in predicting one-time quantities and one-point Lagrangian correlations.

The intermittency in the dissipation range increases the curvature of the Lagrangian correlation and increases the rate of decay of the correlation when the Reynolds number is low. When the Reynolds number is high, the separation between the dissipation and inertial ranges becomes wider and the range of scales contributing to the curvature shifts to lower wavenumber, suggesting that the MLRA should then give a better R_L prediction.

It would be very interesting to see the effects of intermittency on the Eulerian and Lagrangian two-point two-time correlations and to examine the sensitivity of the energy transfer to the two-time Lagrangian covariances within the two-point closure theory. Moreover, since the dynamics of the passive vector in the range $k_d < k < K_{max}$ is dominated by nonlocal interactions, it might be possible to loosen the requirement $K_{max}/k_d \geq 2$ by using an effective subgrid-scale model to

drain passive vector energy at a wavenumber k_p such that $k_d < k_p < K_{max}$.

The authors wish to express their thanks to Dr. A. Wray for his help on the Hypercube computations, to Dr. Y. Kaneda for his stimulating discussions and to Dr. R. Kraichnan for his valuable advice. Time on the Intel Hypercube was furnished by the NAS division at NASA Ames Research Center.

REFERENCES

BATCHELOR, G. K. 1959 *J. Fluid Mech.* **5**, 113.

COMTE-BELLOT, G. & CORRSIN, S. 1971 *J. Fluid Mech.* **48**, 273.

CHEN, S. & KRAICHNAN, R. H. 1989 *Phys. Fluid.* **A1**, 2019.

DANNEVIK, W. P., YAKHOT, V. & ORSZAG, S. A. 1987 *Phys. Fluids.* **30**, 2021.

GOTOH, T., KANEDA Y. & BEKKI, N. 1988 *J. Phys. Soc.* **57**, 866.

GOTOH, T. & KANEDA, Y. 1991 to appear in *Phys. Fluids.*

KANEDA, Y. 1981 *J. Fluid Mech.* **107**, 131.

KANEDA, Y. & GOTOH, T. 1991 *Phys. Fluids.* **A3**, 1924.

KRAICHNAN, R. H. 1965 *Phys. Fluids.* **8**, 575.

KRAICHNAN, R. H. 1966 *Phys. Fluids.* **9**, 1728.

KRAICHNAN, R. H. 1968 *Phys. Fluids.* **11**, 945.

SQUIRES, K. D. & EATON, J. K. 1991 *Phys. Fluids.* **A3**, 130.

MCCOMB, W. D.& SHANMUGASUNDARAM, V. 1984 *J. Fluid Mech.* **143**, 95.

ROGALLO, R. S. 1981 *NASA Tech. Memo. 81315.*

SHE, Z., JACKSON, E. & ORSZAG, S. A. 1988 *J. Sci. Comp.* **4**, 407.

YAKHOT, V. & ORSZAG, S. A. 1986 *J. Sci. Comp.* **1**, 3.

YAKHOT, V., ORSZAG, S. A. & SHE, Z. 1989 *Phys. Fluids.* **A1**, 184.

YEUNG, P. K. & POPE, S. B. 1988 *J. Comp. Phys.* **79**, 373.

YEUNG, P. K. & POPE, S. B. 1989 *J. Fluid Mech.* **207**, 531.